NASA TECHNICAL NOTE

NASA TN D-6926

NASA TN D-6926

ANALYTIC PREDICTION OF AIRPLANE EQUILIBRIUM SPIN CHARACTERISTICS

by William M. Adams, Jr.

Langley Research Center
Hampton, Va. 23365

NATIONAL AERONAUTICS AND SPACE ADMINISTRATION • WASHINGTON, D. C. • NOVEMBER 1972

1. Report No.	2. Government Accession No.	3. Recipient's Catalog No.
NASA TN D-6926		

4. Title and Subtitle	5. Report Date
ANALYTIC PREDICTION OF AIRPLANE EQUILIBRIUM SPIN CHARACTERISTICS	November 1972
	6. Performing Organization Code

7. Author(s)	8. Performing Organization Report No.
William M. Adams, Jr.	L-8319
	10. Work Unit No.
9. Performing Organization Name and Address	501-26-04-01
NASA Langley Research Center Hampton, Va. 23365	11. Contract or Grant No.
	13. Type of Report and Period Covered
12. Sponsoring Agency Name and Address	Technical Note
National Aeronautics and Space Administration Washington, D.C. 20546	14. Sponsoring Agency Code

15. Supplementary Notes

16. Abstract

The nonlinear equations of motion are solved algebraically for conditions for which an airplane is in an equilibrium spin. Constrained minimization techniques are employed in obtaining the solution. Linear characteristics of the airplane about the equilibrium points are also presented and their significance in identifying the stability characteristics of the equilibrium points is discussed. Computer time requirements are small making the method appear potentially applicable in airplane design.

Results are obtained for several configurations and are compared with other analytic-numerical methods employed in spin prediction. Correlation with experimental results is discussed for one configuration for which a rather extensive data base was available. A need is indicated for higher Reynolds number data taken under conditions which more accurately simulate a spin.

17. Key Words (Suggested by Author(s))	18. Distribution Statement
Airplane spin prediction Algebraic nonlinear programing solution Stability of spin Airplane design tool	Unclassified – Unlimited

19. Security Classif. (of this report)	20. Security Classif. (of this page)	21. No. of Pages	22. Price*
Unclassified	Unclassified	39	$3.00

*For sale by the National Technical Information Service, Springfield, Virginia 22151

ANALYTIC PREDICTION OF AIRPLANE EQUILIBRIUM SPIN CHARACTERISTICS

By William M. Adams, Jr.
Langley Research Center

SUMMARY

The nonlinear equations of motion are solved algebraically for conditions for which an airplane is in an equilibrium spin. Constrained minimization techniques are employed in obtaining the solution. Linear characteristics of the airplane about the equilibrium points are also presented and their significance in identifying the stability characteristics of the equilibrium points is discussed. Computer time requirements are small making the method appear potentially applicable in airplane design.

Results are obtained for several configurations and are compared with other analytic-numerical methods employed in spin prediction. Correlation with experimental results is discussed for one configuration for which a rather extensive data base was available. A need is indicated for higher Reynolds number data taken under conditions which more accurately simulate a spin.

INTRODUCTION

Modern fighter airplanes tend to have inertia and aerodynamic characteristics which produce unsatisfactory handling qualities and stability near the stall that can lead to inadvertent entry into the post stall/spin region during maneuvers at high angles of attack. In some cases a steady developed spin can result unless correct recovery techniques are promptly initiated. More than 200 fighter and trainer airplanes were lost in post stall/spin accidents during the period from 1966 to 1970 at a cost of more than 360 million dollars in airplanes and more than 100 fatalities (ref. 1).

Experimental studies of the spin characteristics of airplanes involving tests of dynamically scaled models have been made at the Langley Research Center for a number of years and yield valuable information. The accuracy of the data obtained is limited, however, and some parameters of interest are not measured. Scale effects such as critical Reynolds number differences can make extrapolation of results to the full-scale airplane difficult.

Analytical techniques offer the possibility of spin analyses early in the design process that could provide information complementary to that obtained experimentally. Analytical methods currently employed in spin prediction fall into two categories. One type gains the capability of at-the-desk determination of approximate solutions by either neglecting the effects of some parameters or requiring that only part of the conditions for an equilibrium spin be satisfied (refs. 2, 3, and 4). The second type begins with conditions hopefully either near the spin or favoring development of a spin and integrates the equations of motion forward in time until the average values of the variables are approximately constant (refs. 5 to 8). Such integrations can require considerable amounts of computer time, and residual oscillations in the variables usually necessitate estimation of the equilibrium conditions for steady spins. In some cases persisting oscillations seen with this method may allow identification of a spin as being oscillatory rather than steady.

An analytical technique allowing algebraic determination of airplane equilibrium spin conditions is presented in this paper which is limited in accuracy only by the mass, inertia, and aerodynamic data available. Numerical integration is avoided by casting the problem in a form requiring a constrained minimization solution of a nonlinear function of several variables. Solutions are obtained by using a method for finding a local minimum developed by Davidon (ref. 9) and modified by Fletcher and Powell (ref. 10). Results are presented for several configurations and are compared with other analytical predictions. Correlation with experimental results is discussed for one configuration for which an extensive set of aerodynamic data was available.

Linearized equations of motion are also developed to provide information about the stability of the equilibrium spin conditions. A limited investigation is made of the characteristics of the system about the equilibrium solutions.

SYMBOLS

Values are given in both SI and U.S. Customary Units. The measurements and calculations were made in U.S. Customary Units.

A,B matrices in linearized state equation $\dot{\xi} = A\xi + Bu$

A_V,B_V,C_V coefficients of a quadratic equation, defined in appendix B

A_X,A_Y,A_Z body axis components of aerodynamic forces divided by mV

$a_X = A_X + G_X$, $a_Y = A_Y + G_Y$, $a_Z = A_Z + G_Z$

b	wing span
$\bar{c}$	mean aerodynamic chord
$\vec{F}$	external force on airplane (vector sum of aerodynamic and gravitational forces)
f	vector of nonlinear functions yielding $f^T = (\dot{\alpha},\dot{\beta},\dot{p},\dot{q},\dot{r})$
G	vector of nonlinear functions yielding $G^T = (\dot{\alpha},\dot{\beta},\dot{V},\dot{p},\dot{q},\dot{r})$
G_X,G_Y,G_Z	body axis components of gravity force divided by mV
g	acceleration due to gravity (assumed constant), 9.80665 m/sec^2 (32.174 ft/sec^2)
h	airplane altitude above earth's surface
I_X,I_Y,I_Z,I_{XZ}	body axis moments and product of inertia about the center of mass
J	function to be minimized in order to find an equilibrium spin condition, f^Tf
M_X	rolling moment acting about X body axis
M_Y	pitching moment acting about Y body axis
M_Z	yawing moment acting about Z body axis
m	mass of airplane
p,q,r	angular rates about body axes
q_∞	dynamic pressure, $\frac{1}{2}\rho V^2$
R	radius of helical path of airplane
$\hat{R},\hat{T},\hat{Z}_I$	unit vectors in cylindrical coordinates; $\hat{Z}_I$ is directed toward center of earth (fig. 1)

S	wing area
T_X, T_Y, T_Z	torque components expressed in body axes and divided by the corresponding moment of inertia, $T_X = \frac{\text{x-component of torque}}{I_X}$
T_1, T_2	matrices displaying coordinate system transformations (see appendix A)
t	time
t^*	time at which search for equilibrium solution is made
t_o	initial or reference time in linearized equations of motion
U	control vector, $U^T = (\delta_e, \delta_a, \delta_r)$
u	deviation from nominal control vector, $U(t) - U_N(t)$
u,v,w	body axis components of $\vec{V}$
V	airspeed
W	weight
X,Y,Z	axes
x,y,z	position triple (when devoid of subscripts, a body-axis coordinate system is referred to)
α	angle of attack
β	angle of sideslip
γ	flight-path angle, $\tan^{-1}\left(\frac{\dot{h}}{V}, \frac{V_H}{V}\right)$
$\delta_e, \delta_a, \delta_r$	elevator, aileron, and rudder deflections (positive δ_e is trailing edge down, positive δ_a is right trailing edge down, positive δ_r is trailing edge left)

$\eta^T = (\theta, \phi, \gamma, \omega, \psi')$

$\lambda_1,\lambda_2,\ldots,\lambda_8$ characteristic roots of linearized equations

$\Xi^T = \left(\alpha,\beta,\frac{V}{V_o},p,q,r,\theta,\phi\right)$

ξ deviation from nominal value of Ξ

ρ atmospheric density

ψ,θ,ϕ angles defining transformation between inertial and body axes (see appendix A)

ψ' angle from horizontal projection of airplane longitudinal axis to horizontal component of $\vec{V}$ (positive clockwise when looking up)

ω angular rate about center of mass, $\sqrt{p^2 + q^2 + r^2}$

Subscripts:

H horizontal component

I referred to inertial axis system

IND reading at boom attached to nose of model

N evaluated on nominal flight path

o evaluated at time t_o

S stall angle

w referred to wind axis system

Special symbols:

$(\hat{})$ unit vector

$(\vec{})$ vector

$(\dot{})$ derivative with respect to time

$( )^T$ transpose of matrix

$( )^*$ value which minimizes J

$\{ \}$ column vector

Coefficients and derivatives:

Results presented herein are given in terms of the aerodynamic coefficients and their derivatives defined in the tabulations that follow:

Rolling moment
$C_l = \frac{M_X}{q_\infty Sb}$
$C_{l_{\delta_a}} = \frac{\partial C_l}{\partial \delta_a}$
$C_{l_{\delta_e}} = \frac{\partial C_l}{\partial \delta_e}$
$C_{l_{\delta_r}} = \frac{\partial C_l}{\partial \delta_r}$
$C_{l_p} = \frac{\partial C_l}{\partial \frac{pb}{2V}}$
$C_{l_r} = \frac{\partial C_l}{\partial \frac{rb}{2V}}$
$C_{l_{\dot\beta}} = \frac{\partial C_l}{\partial \frac{\dot\beta b}{2V}}$

Yawing moment
$C_n = \frac{M_Z}{q_\infty Sb}$
$C_{n_{\delta_a}} = \frac{\partial C_n}{\partial \delta_a}$
$C_{n_{\delta_e}} = \frac{\partial C_n}{\partial \delta_e}$
$C_{n_{\delta_r}} = \frac{\partial C_n}{\partial \delta_r}$
$C_{n_p} = \frac{\partial C_n}{\partial \frac{pb}{2V}}$
$C_{n_r} = \frac{\partial C_n}{\partial \frac{rb}{2V}}$
$C_{n_{\dot\beta}} = \frac{\partial C_n}{\partial \frac{\dot\beta b}{2V}}$

Side force
$C_Y = \frac{\left(\vec{F} - m\vec{g}\right) \cdot \hat{y}}{q_\infty S}$
$C_{Y_{\delta_a}} = \frac{\partial C_Y}{\partial \delta_a}$
$C_{Y_{\delta_e}} = \frac{\partial C_Y}{\partial \delta_e}$
$C_{Y_{\delta_r}} = \frac{\partial C_Y}{\partial \delta_r}$
$C_{Y_p} = \frac{\partial C_Y}{\partial \frac{pb}{2V}}$
$C_{Y_r} = \frac{\partial C_Y}{\partial \frac{rb}{2V}}$

Pitching moment	Longitudinal force	Z body axis force component
$C_m = \frac{M_Y}{q_\infty S \bar{c}}$	$C_X = \frac{(\vec{F} - m\vec{g}) \cdot \hat{x}}{q_\infty S}$	$C_Z = \frac{(\vec{F} - m\vec{g}) \cdot \hat{z}}{q_\infty S}$
$C_{m_{\delta_e}} = \frac{\partial C_m}{\partial \delta_e}$	$C_{X_{\delta_e}} = \frac{\partial C_X}{\partial \delta_e}$	$C_{Z_{\delta_e}} = \frac{\partial C_Z}{\partial \delta_e}$
$C_{m_q} = \frac{\partial C_m}{\partial \frac{q\bar{c}}{2V}}$		

PROBLEM FORMULATION AND SOLUTION

Equilibrium Spin Requirements

An algebraic method of solving for airplane equilibrium spin conditions which utilizes nonlinear programing techniques is discussed in this section. The solutions obtained satisfy the requirements of a steady developed spin if the equilibrium points are stable. Solutions that have linear representations that are unstable either correspond to oscillatory spin conditions or are not actual developed spin conditions.

An airplane in an equilibrium spin has the following characteristics:

(1) It is operating in the post stall region

(2) Descent occurs in a helical path about a vertical axis

(3) The axis of the helix, its radius, and the descent speed would remain constant were it not for atmospheric density variation with altitude and other disturbances

Three coordinate systems are employed in this analysis:

(1) An inertial system with origin on the axis of the helix at an altitude h (positive Z-axis downward)

(2) A system fixed in the body with origin at the center of mass

(3) A wind axis system having origin at the center of mass with X_w alined with the airplane velocity vector

The transformations connecting these coordinate systems are given in appendix A.

Having defined the necessary coordinate systems one can state the equilibrium conditions mathematically as follows. Figure 1 will aid in the interpretation of some of the terms.

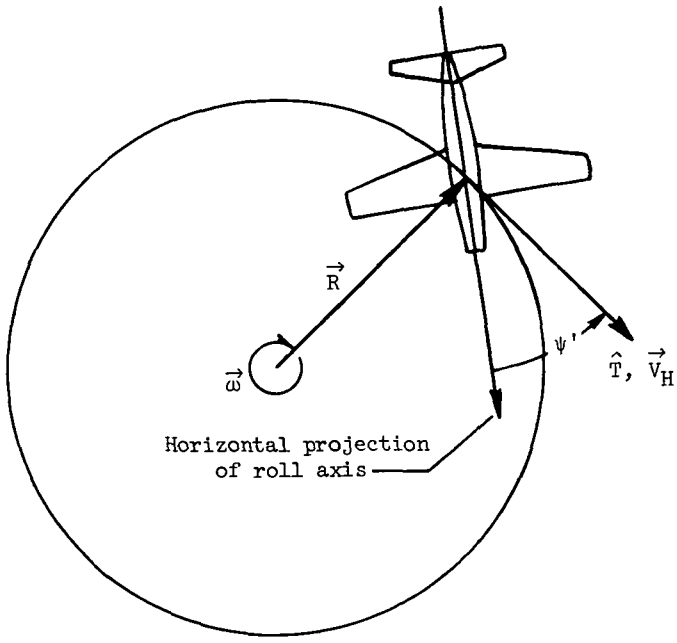

Figure 1.- Top view of helical path.

$$\alpha > \alpha_S \qquad \text{(Airplane is in post stall region)} \tag{1}$$

$$\vec{\omega} = \dot{\psi}\hat{Z}_I \qquad \left(\begin{array}{c}\text{Angular velocity of airplane about its}\\ \text{center of mass is vertical}\end{array}\right) \tag{2}$$

$$\vec{V} = R\dot{\psi}\hat{T} - \dot{h}\hat{Z}_I \qquad \left(\begin{array}{c}\text{Helical path with helix radius such that}\\ R = \dfrac{V_H}{|\dot{\psi}|}, \text{ where } \hat{T} = \hat{Z}_I \times \hat{R}\end{array}\right) \tag{3}$$

$$\vec{\dot{\omega}} = \begin{Bmatrix}\dot{p}\\ \dot{q}\\ \dot{r}\end{Bmatrix} = \{0\} \qquad \text{(Constant angular velocity)} \tag{4}$$

$$\vec{F} = -mR\omega^2\hat{R} \qquad \text{(Helical motion persists)} \tag{5}$$

Expressing the forces in the wind axis system and solving for $\dot{\alpha}$, $\dot{\beta}$, and $\dot{V}$ in equation (5) allow equations (4) and (5) to be written in the form

$$\begin{Bmatrix} \dot{\alpha} \\ \dot{\beta} \\ \dot{V} \\ \dot{p} \\ \dot{q} \\ \dot{r} \end{Bmatrix} = \{0\} \tag{6}$$

Search for an equilibrium spin condition is made at a particular time point t^*. The unconstrained airplane has six degrees of freedom with second-order equations of motion; therefore, 12 parameters are required to completely specify its state at a given instant. However each independent equality constraint imposed upon the system can remove one parameter. This fact is employed in the search for an equilibrium condition to reduce the number of parameters to be searched over. The search is made at a specified altitude h^* and is limited to regions where $\dot{V} = 0$. In addition, search is made only in regions that satisfy the conditions stipulated in equations (2) and (3) by including these four equality constraints explicitly. Finally, the orientation of the horizontal inertial axes is assumed to be such that $\psi(t^*) = 0$. The dimension of the state space to be searched over is, therefore, reduced from 12 to 5 if each control surface is held in a fixed position.

For convenience the set of variables to be searched over was chosen to be $\{\theta,\phi,\gamma,\omega,\psi'\}$. See figure 1 and the symbols for a definition of ψ'.

The equations of motion are presented in appendix B as are the consequences of explicitly satisfying the equality constraints at each point. Engine thrust terms are not included. Earlier studies have indicated that these effects tend to be small and inconsistent in the spinning region; use of thrust in this region is normally avoided since serious engine damage can result and flameouts are likely (refs. 11, 12, and 13).

Solution for conditions satisfying the additional relations in equations (6) is required. Define

$$\eta \equiv \begin{Bmatrix} \theta \\ \phi \\ \gamma \\ \omega \\ \psi' \end{Bmatrix} \qquad \text{and} \qquad f \equiv \begin{Bmatrix} \dot{\alpha} \\ \dot{\beta} \\ \dot{p} \\ \dot{q} \\ \dot{r} \end{Bmatrix}$$

From appendix B it can be seen that satisfying $f = \{0\}$ requires the simultaneous solution of five coupled nonlinear equations involving tabulated aerodynamic data. Only a numerical solution is possible and there is no guarantee that a solution will exist. The procedure employed in this report attempts to solve the following equivalent problem. Find η^* such that

$$J(\eta) = \sum_{i=1}^{5} f_i^2 = \dot{\alpha}^2 + \dot{\beta}^2 + \dot{p}^2 + \dot{q}^2 + \dot{r}^2$$

has a local minimum at $\eta = \eta^*$ while requiring that search be limited to the subspace within which the following equality constraints are satisfied:

$$\psi(t^*) = 0$$

$$h = h^* \qquad \text{(A specified constant)}$$

$$\vec{\omega}(\eta) = \dot{\psi}\hat{Z}_I \qquad \left(\text{i.e., } \omega_{x_I} = \omega_{y_I} = 0\right)$$

$$\dot{V}(\eta) = 0 \qquad \left(V(\eta) \text{ is determined such that } \dot{V}(\eta) = 0 \text{ (see appendix B)}\right)$$

$$\vec{V}(\eta) = R\dot{\psi}\hat{T} - \dot{h}\hat{Z}_I \qquad \left(\text{i.e., } \left(\vec{V} \cdot \hat{R}\right) = 0 \text{ and } R = \frac{V_H}{|\dot{\psi}|}\right)$$

If $\alpha^* > \alpha_S$ and $J(\eta^*) = 0$, an equilibrium solution has been found.

As formulated for this problem, a solution is obtained in an iterative manner beginning with an initial estimate η_1. The method of search is initially equivalent to a gradient or steepest descent procedure, but second-order information is accumulated during the iterations and quadratic convergence is approached near the end of the iterations. Thus, the method has initially the sureness of convergence toward a local minimum of a gradient procedure. Terminally the rapidness of convergence of a second-order method is approached without the necessity of computing and inverting the matrix of second partial derivatives at each point. Details of the method are presented in references 9, 10, and 14. Reference 14 also includes an extension to inequality constraints and is the paper most nearly describing the methods employed in the computer program that was modified for this study.

The procedure developed in this report will henceforth be called a function minimization technique. The solution η^* which minimizes $J(\eta)$ is a local one. Additional equilibrium spin solutions may exist for the same control settings that would be found if a different initial estimate were chosen. In fact two solutions were usually found for a given control setting if one was found. These two solutions are identified as flat and steep spins with the flat spin having the more nearly horizontal longitudinal axis. Inverted spins were not investigated due to lack of aerodynamic data at negative angles of attack.

The solutions found by using the function minimization technique involve no approximations other than those present in the data. Therefore, given sufficiently realistic mass, aerodynamic, and moment of inertia data, the solutions obtained would represent actual

airplane equilibrium spin conditions. The stability of these solutions must be examined, however, to determine whether they represent developed spin conditions one might expect to approximately maintain in a model or flight test.

System Linearized About an Equilibrium Spin Condition

A linearized representation of the airplane equations of motion is developed in order to obtain some information about the stability of the equilibrium spin conditions. Density variation with altitude is neglected. Define $\Xi(t)$ such that

$$\Xi^T(t) = \left(\alpha, \beta, \frac{V}{V_o}, p, q, r, \theta, \phi\right)$$

where

$$\dot{\Xi}(t) = G\left[\Xi(t), U(t)\right]$$

to first order

$$\dot{\xi}(t) = \dot{\Xi}(t) - \dot{\Xi}_N(t) = \left(\vec{\nabla}_{\Xi} G\right)_N^T \xi + \left(\vec{\nabla}_U G\right)_N^T \left[U(t) - U_N(t)\right]$$

or

$$\dot{\xi}(t) = A(t)\ \xi(t) + B(t)\ u(t)$$

The elements of the matrices A and B are presented in appendix C. It is assumed subsequently that $\Xi_N(t)$ corresponds to an equilibrium spin condition with fixed nominal controls in which case A and B are constant matrices.

All stable roots for the linear representation indicates a return to the equilibrium spin conditions for sufficiently small deviations therefrom. Additional analysis would be required to determine whether a solution with an unstable linear representation is an oscillatory or a no-spin solution.

Mass, Inertia, and Dimensional Characteristics

Sketches of the planforms of the configurations studied are shown as figure 2. Configuration A represents a swept-wing fighter, configuration B represents a delta-wing fighter, configuration C represents a supersonic trainer, configuration D represents a stub-wing research vehicle, and configuration E represents a twin-jet swept-wing fighter.

The weight, inertia and dimensional characteristics of the various configurations are shown in table I. These data were taken from references 6, 7, 8, 13, and 15 to 21.

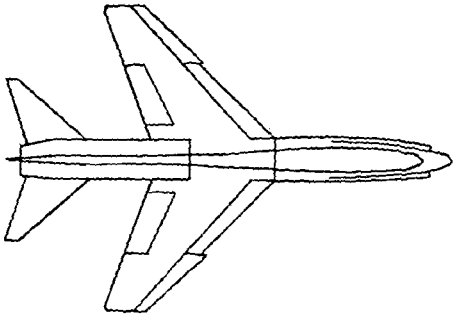

Configuration A

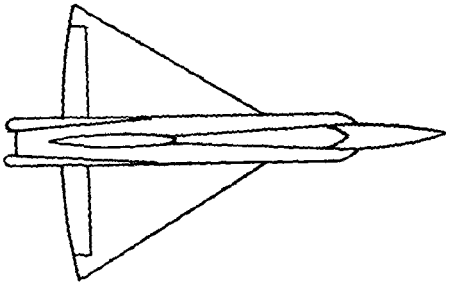

Configuration B

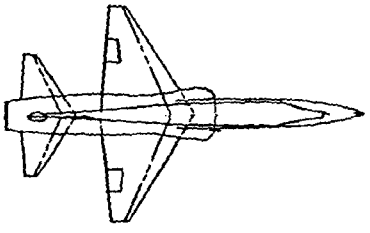

Configuration C

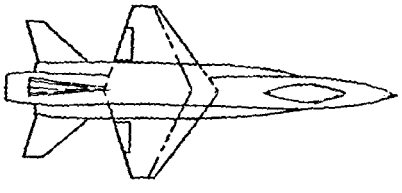

Configuration D

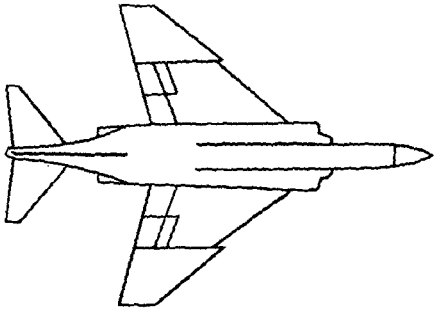

Configuration E

Figure 2.- Plan views of configurations.

TABLE I.- WEIGHT, INERTIA, AND GEOMETRIC CHARACTERISTICS

Configuration	Prediction method (a)	W, N (lb)	I_X, kg-m^2 (slug-ft^2)	I_Y, kg-m^2 (slug-ft^2)	I_Z, kg-m^2 (slug-ft^2)	I_{XZ}, kg-m^2 (slug-ft^2)	S, m^2 (ft^2)	b, m (ft)	$\bar{c}$, m (ft)	Center of mass, percent $\bar{c}$	Control deflection limits			Reference
											δ_e, deg	δ_a, deg	δ_r, deg	
A	S, I, E, M	105 739	15 875	112 060	120 985	0	35.80	10.87	3.61	33	-30 to 10	±15	±6	7, 8, 15
		(23 771)	(11 709)	(82 654)	(89 237)	(0)	(385.55)	(35.67)	(11.83)					
E	F	150 000 to 180 000	-------	-------	-------	---	50.01	11.71	4.8895	29 to 33	-21 to 9	±30	±30	16
		(33 000 to 40 000)					(538.34)	(38.41)	(16.04)					
E	S	161 594	35 397	157 574	178 457	0	50.01	11.71	4.8895	33.9	-21 to 9	±30	±30	17
		(36 328)	(26 108)	(116 222)	(131 625)	(0)	(538.34)	(38.41)	(16.04)					
E	S	156 221	27 832	152 225	172 780	0	50.01	11.71	4.8895	29.6	-21 to 9	±30	±30	18
		(35 120)	(20 568)	(112 277)	(127 438)	(0)	(538.34)	(38.41)	(16.04)					
E	S	159 659	30 674	162 593	184 478	0	50.01	11.71	4.8895	32.4	-21 to 9	±30	±30	18
		(35 893)	(22 624)	(119 928)	(136 066)	(0)	(538.34)	(38.41)	(16.04)					
E	S	165 922	28 148	169 826	193 146	0	50.01	11.71	4.8895	35.8	-21 to 9	±30	±30	18
		(37 301)	(20 761)	(125 259)	(142 459)	(0)	(538.34)	(38.41)	(16.04)					
E	S	154 064	31 944	161 994	183 001	0	50.01	11.71	4.8895	31.9	-21 to 9	±30	±30	19
		(34 635)	(23 561)	(119 481)	(134 975)	(0)	(538.34)	(38.41)	(16.04)					
E	D													20
E	M	160 968	35 398	157 576	178 460	0	50.01	11.71	4.8895	33.3	-21 to 9	±30	±30	
		(36 187)	(26 108)	(116 222)	(131 625)	(0)	(538.34)	(38.41)	(16.04)					
B	I, E	110 365	18 438	173 539	187 096	0	64.57	11.62	7.24	30.0	-25 to 10	±7.5	±25	7, 8
		(24 811)	(13 600)	(128 000)	(138 000)	(0)	(695.05)	(38.12)	(23.755)					
B	M	110 365	18 438	173 539	187 096	5884	64.57	11.62	7.24	30.0	-25 to 10	±7.5	±25	
		(24 811)	(13 600)	(128 000)	(138 000)	(4340)	(695.05)	(38.12)	(23.755)					
C	F	56 270	-------	-------	-------	----	15.79	7.70	2.36	21.5	-17 to 8	±60	±6	13
		(12 650)					(170)	(25.25)	(7.73)					
C	I, E, M	44 653	2 305	39 995	40 800	----	15.79	7.70	2.36	21.5	-15 to 5	±60	±6	8
		(10 038)	(1 700)	(29 500)	(30 100)		(170)	(25.25)	(7.73)					
D	D, I, E, M	55 936	5 814	99 462	101 502	0	18.58	6.82	3.13	19.5	-30	±7.5	±7.5	6, 21
		(12 575)	(4 228)	(73 384)	(74 867)	(0)	(200)	(22.36)	(10.27)					

[a] F, flight test; D, drop test; S, spin tunnel; I, numerical integration; E, estimation method; M, function minimization.

Aerodynamic data for configuration E were taken from references 22 and 23. Data representing the aerodynamics of configuration B were taken from reference 24. All other aerodynamic data were taken from reference 8 which contains a compilation of data for several configurations. Other references that present aerodynamic data for configurations A, B, C, and D and discuss the manner in which some parameters were estimated include references 5, 6, 21, 25, and 26.

The dynamic derivatives data used in this study contain several approximations:

(1) The measured values taken for the dynamic derivatives include other inseparable terms $\left(\text{e.g., } C_{l_p} \text{ actually is } C_{l_p} + C_{l_{\dot\beta}} \sin\alpha,\ C_{n_r} \text{ is actually } C_{n_r} - C_{n_{\dot\beta}} \cos\alpha, \text{ etc.}\right)$. See reference 23 for more discussion of the difficulties.

(2) For all configurations other than E, constant values of C_{m_q} were used. These correspond to the values employed in reference 8 for configurations A, C, and D and to the value employed in reference 24 for configuration B.

RESULTS AND DISCUSSION

Equilibrium spin conditions predicted by using the function minimization technique are presented. These results are compared with other analytic predictions. Comparisons are made between experimental test results and function minimization predictions

for configuration E and they indicate a need for additional aerodynamic data. A limited investigation is made of the stability of the equilibrium spin conditions predicted by function minimization.

Equilibrium Spin Predictions

Experimental spin test results for configurations A, B, C, and D are presented in references 5, 6, 13, 15, 16, and 21. Explicit comparisons are not made herein between these experimental results and the function minimization predictions. The reader who makes such correlations is cautioned to give careful consideration to the fact that some of the aerodynamic data were estimated for these configurations possibly in such a manner as to favorably affect the correlations.

In tables II to IV, spin condition predictions are compared which were obtained by using the function minimization technique, a numerical integration procedure, and the analytical estimation procedure presented in reference 4. The numerical integration procedure begins with conditions thought to be near the developed spin and then the equations of motion are integrated forward in time until the average values of α and $\dot{\psi}$ are approximately constant. The estimation procedure assumes that spinning occurs at wings level flight ($\beta = \phi = 0$) and requires only that $\dot{q}$ and $\dot{r}$ be zero and that the velocity be such that the drag balances the gravity force.

Configuration A.- Table II indicates that, for configuration A, the average values of α, β, and ω found by numerical integration correspond quite closely with those predicted by function minimization. The smaller value of V predicted by numerical integration is of little significance being due to a difference in atmospheric density. The integration was initiated at an altitude of 9144 m (30 000 ft), but equilibrium conditions were approached at some lower altitude where the atmosphere was more dense. Consequently a smaller velocity was required to obtain a balance between aerodynamic and gravity forces.

TABLE II.- SPIN CHARACTERISTICS FOR CONFIGURATION A

[Altitude, 9144 m (30 000 ft)]

Prediction method	δ_e, deg	δ_a, deg	δ_r, deg	α, deg	β, deg	V, m/sec (ft/sec)	ω, rps	θ, deg	ϕ, deg	R, m (ft)	ψ', deg
Function minimization	-30	5	-6	77.05	-1.483	84.70 (277.9)	0.3900	-12.92	-0.8413	0.3996 (1.311)	-87.72
Numerical integration[a]	-30	5	-6	73 to 81	-6 to 3	77.40 (254)	.39				
Estimation	-30	5	-6	59	0	94.7 (311)	.27	-31	0		
Function minimization	-30	15	-6	83.60	-.9154	82.94 (272.1)	.5631	-6.394	-.6806	.09778 (.3208)	-87.77

[a]Reference 7.

The approximate analytic procedure predicted a lower spin rate and a much steeper spin with a higher value of V than that found by the function minimization technique.

Configuration B.- Predicted spin characteristics of configuration B are shown in table III. Flat spin prediction by numerical integration beginning with an initial altitude of 9144 m (30 000 ft) is in good agreement with the function minimization prediction for α and β and yields a slightly higher value of ω (0.22 rps vs 0.1910 rps). The difference in V between these two methods is again mainly due to the altitude loss that occurred during the time history generation.

The analytic estimation method also predicts flat spin characteristics that are near the function minimization values for α, ω, and V.

The steep spin predicted by the estimation procedure is slightly flatter and faster than that found by function minimization. Other steep spins predicted by function minimization are also shown. The spin rates are generally considerably lower than the flat spin rates. The zero control deflection solution shown is quite near the stall angle of attack and is highly unstable.

TABLE III.- SPIN CHARACTERISTICS FOR CONFIGURATION B

[Altitude, 9144 m (30 000 ft)]

Prediction method	Type of spin	δ_e, deg	δ_a, deg	δ_r, deg	α, deg	β, deg	V, m/sec (ft/sec)	ω, rps	θ, deg	ϕ, deg	R, m (ft)	ψ', deg
Function minimization	Flat	-25	7.5	-25	73.63	-2.410	78.36 (257.1)	0.1910	-16.40	-0.4650	2.238 (7.342)	-91.02
Numerical integration[a]	Flat	-25	7.5	-25	75	-2.0	66.8 (219)	.22				
Function minimization	Flat	-25	7	-25	73.21	-2.383	78.55 (257.7)	.1875	-16.81	-.3650	2.366 (7.763)	-90.70
Estimation	Flat	-25	7	-25	69	0	77.4 (254)	.16	-21	0		
Function minimization	Flat	0	0	0	65.83	-1.960	79.40 (260.5)	.1857	-24.07	.9331	3.340 (10.96)	-87.54
Function minimization	Steep	-25	7	-25	49.56	-2.978	94.95 (311.5)	.08234	-38.92	7.733	28.93 (94.98)	-77.06
Estimation	Steep	-25	7	-25	55	0	87.2 (286)	.095	-35	0		
Function minimization	Steep	-25	7	0	49.18	-3.161	95.25 (312.5)	.08164	-39.33	7.665	29.57 (97.03)	-77.39
Function minimization	Steep	-25	0	-25	59.15	-1.225	88.45 (290.2)	.1239	-30.24	4.228	9.720 (31.89)	-81.57
Function minimization	Steep	0	0	0	35.59	-9.395	98.12 (321.9)	.1743	-54.35	-3.772	11.22 (36.82)	-93.09

[a]Reference 7.

Configuration C.- Since the same aerodynamic model and moments of inertia, and so forth, were assumed in each case for configuration C, the numerical integration and function minimization predictions shown in table IV(a) should have been close. (The speed V was not given.) A relatively large difference is seen in spin rate however. From examination of figure 12 of reference 8 it appears that the spin rate could have still been building up when recovery controls were applied. Thus, with the numerical integration procedure, one can be mistaken about the location of a steady spin if a momentary hesitation in $\dot{\psi}$ occurs while the general trend is toward increasing $\dot{\psi}$. To avoid such errors it would be necessary, generally, to perform the integrations for a longer period to be certain that steady conditions had been reached.

The estimation procedure predicts a steeper spin (73° vs 83.71°) and a smaller spin rate (0.32 rps vs 0.5442 rps) than that found by function minimization.

TABLE IV.- FLAT SPIN CHARACTERISTICS FOR CONFIGURATIONS C AND D

Prediction method	δ_e, deg	δ_a, deg	δ_r, deg	α, deg	β, deg	V, m/sec (ft/sec)	ω, rps	θ, deg	ϕ, deg	R, m (ft)	ψ', deg
(a) Configuration C; altitude, 12 192 m (40 000 ft)											
Function minimization	-15	40	-4	83.71	-1.116	84.76 (277.3)	0.5442	-6.312	-0.8103	0.1343 (0.4406)	-94.17
Numerical integration[a]	-15	40	-4	81.0	-5 to 1		>.46				
Estimation	-15	40	-4	73.0	0	87.2 (286)	.32	-17	0		
(b) Configuration D; altitude, 4572 m (15 000 ft)											
Function minimization	-30	7.5	-7.5	88.0	-2.339	52.2 (171.2)	0.4888	-2.093	-1.913	0.1298 (0.4260)	-103.0
Numerical integration[b]	-30	7.5	-7.5	84 to 89	1 to -8	55.2 (181)	.44				
Estimation	-30	7.5	-7.5	85.0		52.4 (172)	.32	-5	0		

[a]Reference 8.

[b]Reference 7.

Configuration D.- Flat spin predictions for configuration D are shown in table IV(b). Good agreement is seen between numerical integration and function minimization predictions of α, β, and V and about a 10-percent difference in spin rate.

The estimation method predicts a much smaller spin rate than that found by function minimization (0.32 rps vs 0.4888 rps).

Comparison of analytic methods.- The approximate method of reference 4 is fast and easy to use and requires only a desk calculator. It is probably more accurate for flat spins than steep spins. Because only part of the spin conditions are satisfied, the accuracy of a given solution would be difficult to ascertain without results from another

technique. Use of solutions obtained with this method as initial conditions for the numerical integration procedure should reduce the time required for convergence to developed spin conditions.

Spin prediction by numerical integration has several attractive features. Information is obtained about spin entry characteristics, and oscillatory spins can perhaps be distinguished from steady spins by using this method. Unless a good estimate of the spinning condition is available, however, considerable computer time may be required to converge upon the spin conditions. Also, a point where momentary hesitation in the time variation of spin rate occurs can be mistaken for a developed spin solution.

The function minimization technique's convergence to an equilibrium spin solution is relatively insensitive to the initial estimate. The data setup requirements are essentially the same as for a numerical integration. This is the only one of the analytic methods which precisely determines equilibrium conditions which allows constant coefficient linear equations to be written. Steady spin conditions are identified if the characteristic roots of the linear representation are stable. Additional study, possibly employing numerical integration, would be required to determine whether linearly unstable equilibrium spin conditions were oscillatory spins or not actual spins. However, beginning the numerical integrations with conditions only slightly perturbed from the equilibrium conditions should minimize the time required to make this determination. The computer time requirements for obtaining function minimization equilibrium spin solutions are small (on the order of 2 seconds or less of Control Data 6600 central processor time per solution for multiple solution runs). This small time requirement makes the method appear potentially applicable as a design tool for use in evaluating the effects of aerodynamic parameter variations on the spin characteristics of an airplane.

Configuration E.- A number of experimental studies have been made of the spin characteristics of configuration E as can be seen in table V. Results are shown from a flight test and three spin tunnel model tests. These results are compared with function minimization predictions. Radio-controlled model drop tests are described in reference 20.

Six sets of dynamic derivative data were available for configuration E, each of which was measured at one of two amplitudes of oscillation and one of three frequencies of oscillation (ref. 23). A set was chosen that was taken with the largest amplitude of oscillation and a reduced frequency of 0.156. With this rather arbitrary selection, function minimization predictions in table V are seen to be in close agreement with spin tunnel results for the flat spin. A similar agreement was observed between the drop test results and function minimization predictions made under conditions corresponding to those of the drop test.

TABLE V.- SPIN CHARACTERISTICS FOR CONFIGURATION F

[Altitude, 7620 m (25 000 ft) except in flight tests where, e.g., in one of the flat spins 11 000 m (37 000 ft) ≧ h ≧ 3048 m (10 000 ft)]

Prediction method	Type of spin	δ_e, deg	δ_a, deg	δ_r, deg	Center of mass, percent $\bar{c}$	α, deg	β, deg	V, m/sec (ft/sec)	ω, rps	θ, deg	ϕ, deg	R, m (ft)	ψ', deg	Reference
Flight test	Flat	-21	Variable (0 to 15)	-30	29 to 33	82	$5 < \beta_{IND} < 25$		0.22					16
Spin tunnel	Flat	-21	30	-30	30.4	84		83.8 (275)	.54		-8 to 10			17
Spin tunnel	Flat	-21	30	-30	33.9	85		81.4 (267)	.62		1			17
Spin tunnel	Flat	-21	30	-30	29.6	86		79.6 (261)	.54		-4 to 6			18
Spin tunnel	Flat	-21	30	-30	32.4	87		79.6 (261)	.63		-6 to 8			18
Spin tunnel	Flat	-21	30	-30	35.8	88		79.6 (261)	.60		0			18
Spin tunnel	Flat	-21	30	-30	31.9	83		79.9 (262)	.54		+4			19
Function minimization	Flat	-21	30	-30	33.3	81.58	-0.1541	89.18 (292.6)	.5244	-8.694	0.2351	0.2227 (.7307)	-125.1	
Function minimization	Flat	0	0	0	33.3	82.47	.05369	87.81 (288.1)	.5903	-7.804	.3185	.1562 .5126)	-136.1	
Spin tunnel	Flat	-21	0	-30	30.4	80		87.2 (286)	.47		-6 to 5			17
Spin tunnel	Flat	-21	0	-30	33.9	85		87.2 (286)	.50		-4 to 3			17
Spin tunnel	Flat	-21	0	-30	31.9	82		79.4 (262)	.52		-6 to 6			19
Function minimization	Flat	-21	0	-30	33.3	82.24	.1450	88.75 (291.7)	.5469	-8.030	.5000	.1997 (.6552)	-127.6	
Flight test	Steep	≈-21	Variable	≈-30	29 to 33	60			.11 to .17					16
Spin tunnel	Steep	-21	30	-30	31.9	46 to 58		104 (342)	.19		-12 to 14			19
Spin tunnel	Steep	-21	30	-30	29.6	58 to 71		89.9 (295)	.19 to .25		-8 to 10			18
Function minimization	Steep, non-equilibrium	-21	30	-30	33.3	47.99	.9764	109.4 (358.8)	.2273	-41.77	5.939	4.609 (15.12)	-84.59	
Function minimization	Steep	0	0	0	33.3	59.39	-.1513	93.42 (306.5)	.2725	-30.63	2.288	2.019 (6.623)	-89.98	
Function minimization	Intermediate	-21	30	-30	33.3	73.17	.05453	90.98 (298.5)	.3648	-17.01	1.049	.6690 (2.195)	-100.5	
Function minimization	Intermediate	0	0	0	33.3	73.18	-.4839	89.28 (292.9)	.3925	-17.04	.3416	.5316 (1.744)	-105.5	

The steep spin conditions predicted by function minimization lie within the range of oscillations noted in the experimental tests. However, the steep spin solution for control deflections of elevator up, rudder with, and aileron against the spin is a nonequilibrium one $\left(\text{i.e., } \partial J(\eta)/\partial\eta\big|_{\eta=\eta^*} = \{0\} \text{ but } J(\eta^*) \neq 0\right)$. A time history beginning with the non-equilibrium conditions resulted in an oscillatory spin that tended to approach conditions resembling a flat spin.

A spin mode intermediate to the flat and steep spins was also predicted by the function minimization procedure and is shown in table V for two control settings. Such a spin mode for this configuration was noted in the spin tunnel tests described in reference 18.

Subsequent runs with parameters from the other sets of dynamic derivative data generally did not correlate as well with the model test results. The results obtained are shown in table VI. This table indicates that the small amplitude, low angular rate, dynamic derivative data produced by forced oscillation of the model about static positions do not

TABLE VI.- DEPENDENCE OF SPIN CHARACTERISTICS UPON FREQUENCY AND AMPLITUDE OF OSCILLATIONS EMPLOYED IN DYNAMIC DERIVATIVE TESTS

Reduced frequency	Amplitude of oscillation, deg	α, deg	β, deg	V, m/sec (ft/sec)	ω, rps	θ, deg	ϕ, deg	R, m (ft)	ψ', deg
0.109	$\Delta\phi = \pm 5$ $\Delta\psi = \pm 5.25$	86.77	0.9885	87.17 (286.0)	0.9002	-3.496	1.077	0.07526 (0.2469)	-161.9
.156	$\Delta\phi = \pm 5$ $\Delta\psi = \pm 5.25$	No flat equilibrium spin found to the right							
.203	$\Delta\phi = \pm 5$ $\Delta\psi = \pm 5.25$	83.58	.2801	87.66 (287.6)	.6403	-6.678	.4943	.1279 (.4196)	-141.1
.109	$\Delta\phi = \Delta\psi = \pm 10.50$	82.80	.2614	87.72 (287.8)	.6042	-7.472	.5120	.1493 (.4899)	-138.2
.156	$\Delta\phi = \Delta\psi = \pm 10.50$	82.47	.05369	87.81 (288.1)	.5903	-7.804	.3185	.1562 (.5126)	-136.1
.203	$\Delta\phi = \Delta\psi = \pm 10.50$	79.91	-.3203	88.06 (288.9)	.5090	-10.38	.07232	.2322 (.7619)	-125.9

adequately represent the effects of the large amplitude, high angular rate spinning motion upon the aerodynamically produced forces and moments. This view is supported by reference 17 which presents limited experimental rotary-balance test results showing that the aerodynamic forces and moments can be very nonlinear functions of the rate of rotation. Clearly, means of obtaining data which properly exhibit these nonlinear relationships are needed. Rotary-balance testing, described in reference 27, is designed to measure aerodynamic forces and moments with the model rotating at a constant rate. These measurements can be taken with a nonzero spin radius and are made at fixed values of α and β. Data taken by this technique might allow more reliable analytic prediction of model spin characteristics.

Spin angles of attack predicted by model tests correspond closely with those observed in flight tests as do those predicted by function minimization, with the arbitrary set of dynamic derivative data discussed earlier being used. The same correspondence does not hold in spin rate however. The spin rates observed in the flight tests were much less than those found by model testing and function minimization for both flat and steep spins. Some differences are to be expected due to the limited accuracy of model and full-scale test procedures and the inadequacies in the aerodynamic data discussed previously. The large differences seen in table V, however, indicate the possibility that other error sources, such as a critical Reynolds number difference between model and full-scale conditions, are present. The differences are significant since the spin rate is one of the important factors determining the success or failure of spin recovery techniques. Reference 28 describes techniques that have been employed in the Langley spin tunnel to partially compensate for effects of Reynolds number differences. Aerodynamic data obtained in high Reynolds number facilities are essential for analytic purposes if force and moment data exhibit significant Reynolds number dependence in the range between model and full-scale tests.

TABLE VII.- CHARACTERISTIC ROOTS OF LINEAR REPRESENTATIONS

Configuration	h, m (ft)	δ_e, deg	δ_a, deg	δ_r, deg	Type of spin	α, deg	ω, rad/sec	λ_1, λ_2, sec^{-1}	λ_3, λ_4, sec^{-1}	λ_5, λ_6, sec^{-1}	λ_7, sec^{-1}	λ_8, sec^{-1}
A	9 144 (30 000)	-30	5	-6	Flat	77.05	2.454	(-0.128,±3.26)	(-0.0119,±2.76)	(-0.110,±2.44)	(-0.206,0)	(-0.0545,0)
B	9 144 (30 000)	0	0	0	Flat	65.83	1.167	(-0.169,±2.57)	(-0.0476,±1.62)	(-0.121,±1.16)	(-0.147,0.0364)	(-0.147,-0.0364)
B	9 144 (30 000)	0	0	0	Steep	35.59	1.095	(1.34,±1.35)	(-0.959,±1.63)	(-0.0957,±1.10)	(-2.51,0)	(-0.198,0)
B	9 144 (30 000)	-25	7	-25	Flat	73.21	1.178	(-0.161,±2.73)	(-0.0665,±1.75)	(-0.122,±1.17)	(-0.218,0)	(-0.0705,0)
B	9 144 (30 000)	-25	7	-25	Steep	49.56	.5174	(-0.350,±2.35)	(-0.141,±0.908)	(-0.103,±0.518)	(-0.177,0)	(2.39×10^{-7},0)
C	12 192 (40 000)	-15	40	-4	Flat	83.71	3.419	(0.183,±3.84)	(-0.0687,±3.42)	(-0.296,±3.38)	(-0.226,0)	(-0.0349,0)
E	7 620 (25 000)	0	0	0	Flat	82.47	3.709	(-0.0232,±4.02)	(-0.0895,±3.68)	(-0.484,±3.41)	(0.365,0)	(-0.223,0)
E	7 620 (25 000)	0	0	0	Intermediate	73.18	2.466	(0.332,±2.94)	(-0.245,±2.89)	(-0.111,±2.47)	(-0.631,0)	(-0.229,0)
E	7 620 (25 000)	0	0	0	Steep	59.39	1.712	(0.213,±2.48)	(-0.626,±2.10)	(-0.101,±1.71)	(-0.182,0)	(0.155,0)
E	7 620 (25 000)	-21	30	-30	Flat	81.58	3.295	(-0.123,±3.85)	(-0.0996,±3.28)	(-0.433,±3.22)	(0.464,0)	(-0.219,0)
E	7 620 (25 000)	-21	30	-30	Intermediate	73.17	2.292	(-0.124,±2.77)	(0.158,±2.74)	(-0.109,±2.29)	(-0.543,0)	(-0.227,0)
E	7 620 (25 000)	-21	30	-30	Steep, non-equilibrium	48.00	1.428	(0.405,±2.38)	(-0.808,±1.82)	(-0.0897,±1.43)	(-0.140,0)	(3.06×10^{-8},0)

Linear Characteristics

A general development of the linearized equations of motion is presented in appendix C. In this section the linearized representation is utilized to obtain some indication of the stability of the equilibrium spin conditions. A complete stability analysis, which would involve consideration of the stability of nonlinear systems, has not been attempted.

Characteristic roots for the system linearized about equilibrium spin conditions are shown in table VII for several of the configurations studied. A return to the equilibrium conditions is to be expected for sufficiently small initial disturbances from stable equilibrium points. Figure 3 illustrates this type of behavior for the flat spin of configuration B corresponding to control settings of elevator up, aileron against, and rudder with the spin. The time history is generated by using the nonlinear equations of motion and by assuming constant atmospheric density and an initial perturbation of $\Delta q_o = -7.5^o/sec$. The oscillatory behavior and the damping characteristics seen in figure 3 correspond closely, particularly for α, to those of the second largest complex conjugate pair of characteristic roots for this equilibrium spin solution as given in table VII. This indicates that the mode associated with this pair of roots is the dominant one under a perturbation in pitch rate.

Most linear representations shown exhibit one or more unstable roots as seen in table VII and require additional analysis to determine whether the equilibrium point corresponds to a persisting oscillatory spin or whether it is not a developed spin condition. Such an analysis has not been attempted herein; however, limited results are shown in

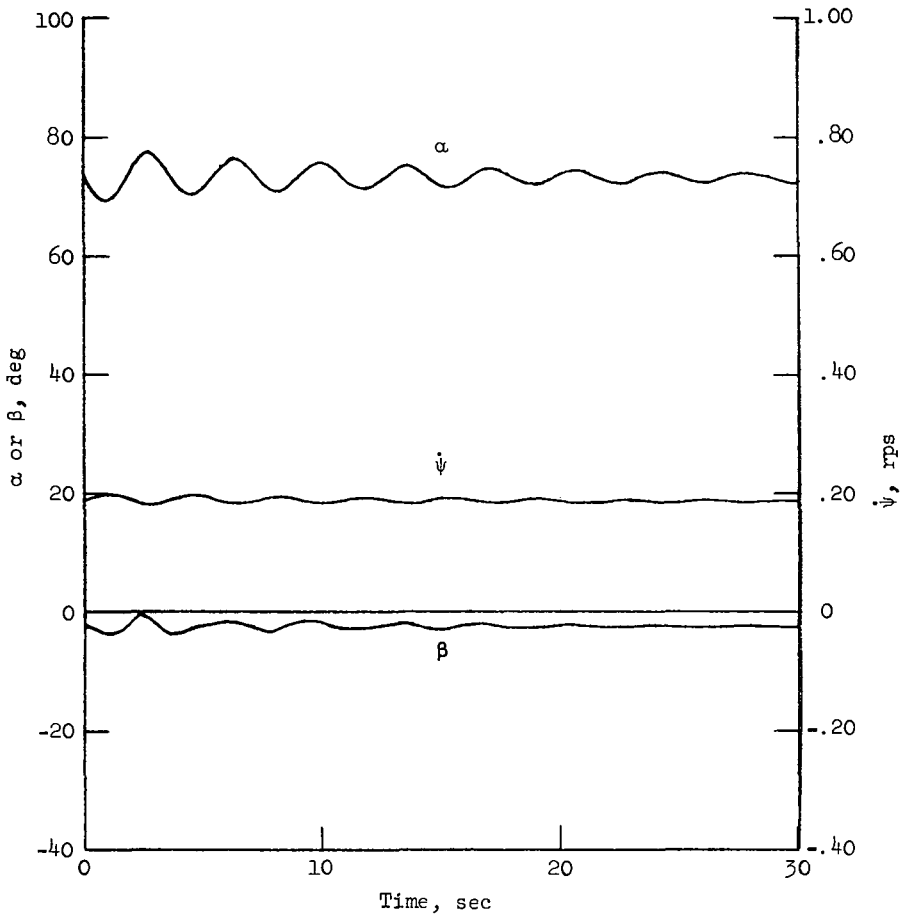

Figure 3.- Time history for configuration B. $\Delta q_o = -7.5^o/sec.$

figure 4 for the flat spin solution found for configuration E for zero control deflections. These time histories are generated by assuming constant atmospheric density and initial conditions perturbed from the equilibrium point by $\Delta q_o = -5^o/sec.$

The solid curves in figure 4(a) are generated by using the nonlinear equations of motion whereas the dashed curves were obtained by using a linear representation. Two sets of linear responses are shown for each parameter, one beginning on the nonlinear trajectory at $t = 0$ with the linear representation about the flat spin and the second beginning on the nonlinear trajectory at $t = 10$ seconds with the linear representation about the intermediate spin. Good qualitative agreement is seen for approximately 10 seconds in each case indicating that the linearized equations of motion may yield an adequate qualitative description of the system's time development over a relatively large region around an equilibrium point.

The results shown in figure 3 and figure 4(a) indicate that the linearized stability characteristics of the equilibrium spin conditions can yield valuable insight into the nonlinear motions of an airplane in the vicinity of these points if the correct aerodynamic

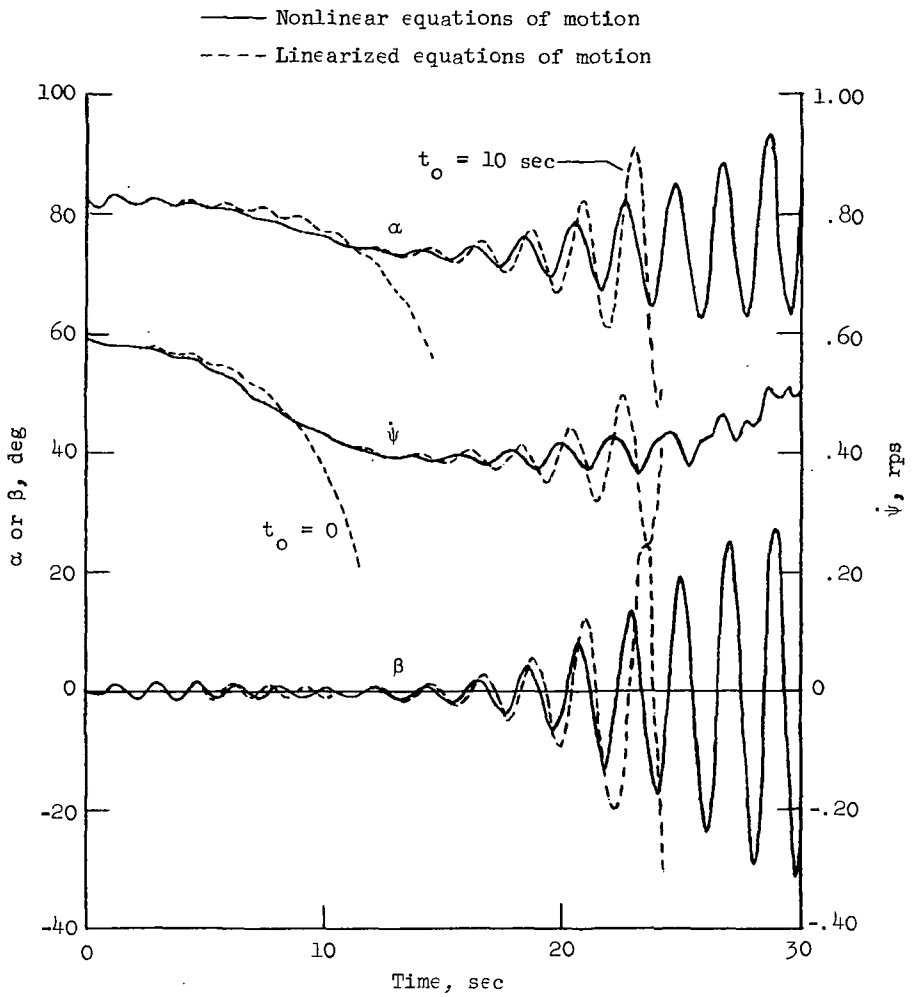

(a) $\Delta q_{t=0} = -5^{\circ}/\text{sec}$.

Figure 4.- Time histories for configuration E.

data in the spin regime can be obtained. Unfortunately the data are often inadequate. For example, flight and model tests of configuration E have demonstrated that the flat spin is stable and virtually steady. This result is in sharp contrast with the flat spin found by using the mathematical model as is seen in figure 4(a) and table VII.

Figure 4(b) illustrates the nonlinear system time development with the same initial conditions as in figure 4(a) for $C_{n_r} = -0.177$ when $\alpha > 80^{\circ}$. The motion, although not steady, diverges much more slowly from the flat spin equilibrium point and illustrates the sensitivity of the dynamic characteristics to the dynamic derivatives. The value of C_{n_r} chosen corresponds approximately both to its value at the equilibrium point and to the rotation balance equilibrium value at $\alpha = 85^{\circ}$ as determined from reference 17.

The dynamic behavior of an airplane is strongly dependent upon its linear stability characteristics. However, other factors must also be considered if a desired dynamic

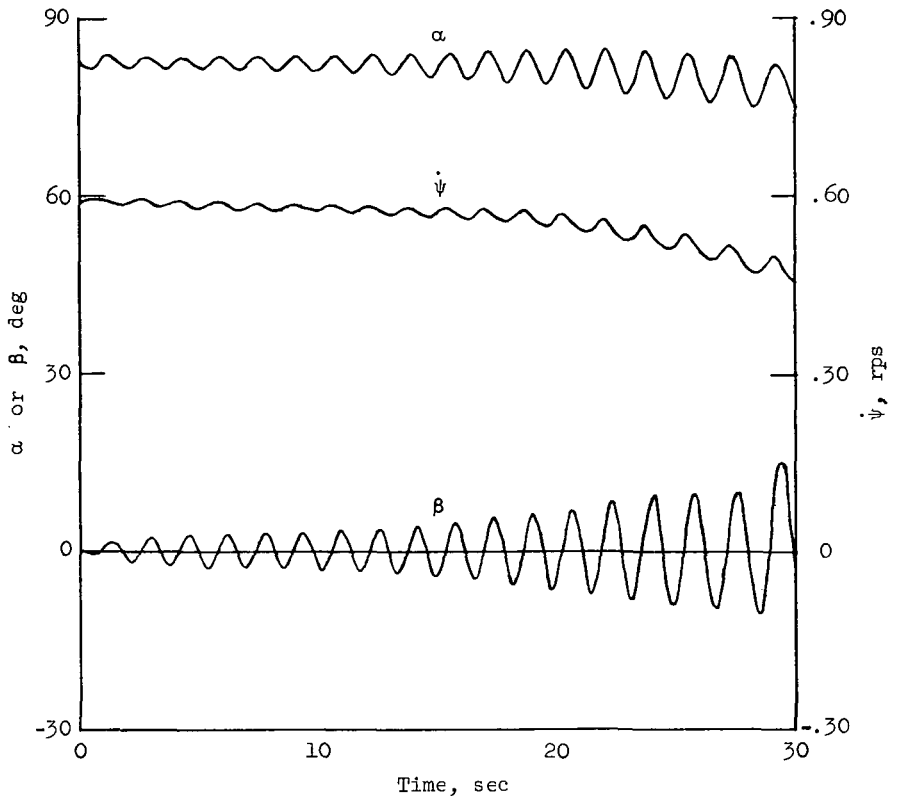

(b) $\Delta q_o = -5°/sec$; $C_{n_r} = -0.177$ for $80° \leq \alpha \leq 90°$.

Figure 4.- Concluded.

response is to be obtained. Thus a linearly unstable equilibrium point does not necessarily indicate that a recovery can be readily achieved. Some factors that could delay or prevent recovery include (1) other equilibrium points may exist in the vicinity, (2) the recovery controls applied may not excite the unstable mode or modes sufficiently, and (3) nonlinear effects may cause the spin to be an oscillatory one which tends to remain within a bounded region in the vicinity of the equilibrium point. One example of this type of behavior is a recovery attempt from the zero control flat spin of configuration E with the control settings often referred to as "optimum recovery controls" (i.e., elevator up, aileron with, and rudder against the spin). Recovery was not achieved after 10 turns despite the tendency to diverge from the equilibrium conditions as discussed previously. The same recovery procedure for the zero control flat spin of configuration B, which is stable, resulted in a recovery in less than two turns; this recovery could be anticipated since no equilibrium spin condition was found for this configuration for full aileron with the spin.

These examples indicate that caution should be exercised when attempting to correlate the stability characteristics of the linearized representation with ease of recovery.

Nevertheless, more detailed analysis of the factors affecting the stability of the equilibrium spin conditions might aid in the design of configurations having more acceptable spin characteristics and identify more destabilizing recovery techniques allowing improved recovery capability. Reference 29 discusses some of the parameters affecting the stability of very flat spins.

CONCLUDING REMARKS

A function minimization method has been demonstrated which will determine exact equilibrium spin conditions for any given inertia and aerodynamic data in the spin region. Linear characteristics of the equilibrium spin conditions are also obtained. Limited analysis indicates that the stability and dynamic characteristics of the linearized representation can yield valuable insight into the nonlinear motion of an airplane in the vicinity of the equilibrium points if the correct aerodynamic data can be obtained.

Application of the method to the prediction of spin characteristics for one configuration for which an extensive data base was available yielded results which correlated well with model tests only when an arbitrary choice was made between available sets of dynamic derivative data. This arbitrariness coupled with incorrect stability characteristics for this configuration's flat spin mode indicates a need for more accurate aerodynamic data taken under conditions which more nearly represent the spinning models. The spin rates observed in flight tests of this configuration did not agree with those found in model tests or with those using data derived from models. The differences are due in part to the limited accuracy of model and full-scale test procedures and to failure to simulate adequately the environment of the spinning model when obtaining aerodynamic data; the large differences seen, however, indicate the possibility that other error sources such as a critical Reynolds number difference between model and full-scale conditions are present.

The method can be employed to aid in the prediction of spin characteristics of future airplanes in the design stage if appropriate analytically or experimentally determined aerodynamic data are available. Computer time requirements per equilibrium spin solution are small in multiple solution cases making the method appear applicable in studying the effect of aerodynamic parameter variations upon the spin characteristics of an airplane.

Comparison of the spin characteristics predicted by function minimization with those observed in flight and model testing can aid in determining the adequacy of the aerodynamic data in the spin region.

Langley Research Center,
National Aeronautics and Space Administration,
Hampton, Va., September 15, 1972.

APPENDIX A

COORDINATE SYSTEM TRANSFORMATIONS

Three sets of coordinate systems are employed in the analysis. The transformations relating the coordinate systems are presented as follows.

(1) Inertial to body axes (angular orientation):

$$\begin{Bmatrix} \hat{x} \\ \hat{y} \\ \hat{z} \end{Bmatrix} = T_1(\psi,\theta,\phi) \begin{Bmatrix} \hat{x}_I \\ \hat{y}_I \\ \hat{z}_I \end{Bmatrix}$$

where ψ (yaw) is counterclockwise rotation about inertial Z_I-axis, θ (pitch) is counterclockwise rotation about resulting Y-axis, and ϕ (roll) is counterclockwise rotation about an axis parallel to X-axis. Figure 5 shows, in three stages, the angular rotations

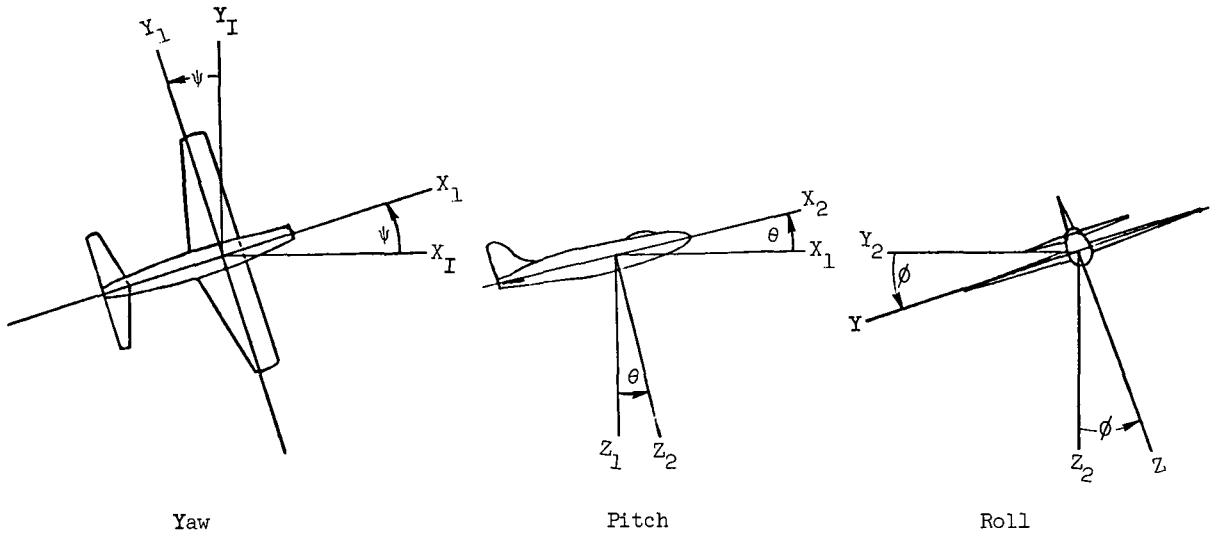

Figure 5.- Inertial to body axes transformation.

defining the transformation. Each view is from a point on the positive axis about which the rotation is taken toward the origin of coordinates.

The matrix $T_1(\psi,\theta,\phi)$ has the following form

$$T_1 = \begin{bmatrix} \cos\psi\cos\theta & \sin\psi\cos\theta & -\sin\theta \\ \cos\psi\sin\theta\sin\phi & \cos\psi\cos\phi & \cos\theta\sin\phi \\ -\sin\psi\cos\phi & +\sin\psi\sin\theta\sin\phi & \\ \cos\psi\sin\theta\cos\phi & \sin\psi\sin\theta\cos\phi & \cos\theta\cos\phi \\ +\sin\psi\sin\phi & -\cos\psi\sin\phi & \end{bmatrix}$$

(2) Body to wind axes (see fig. 6):

$$\begin{Bmatrix} \hat{x}_w \\ \hat{y}_w \\ \hat{z}_w \end{Bmatrix} = T_2(\alpha,\beta) \begin{Bmatrix} \hat{x} \\ \hat{y} \\ \hat{z} \end{Bmatrix}$$

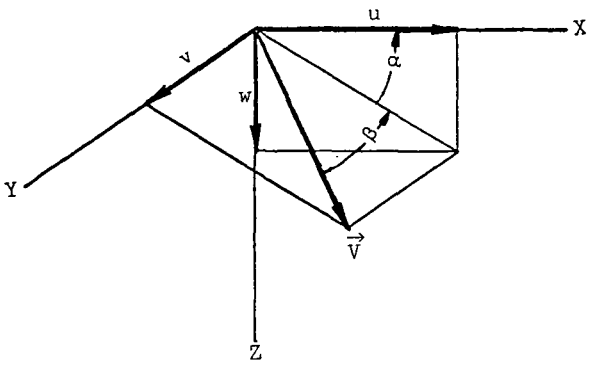

Figure 6.- Wind to body axes transformation.

where α (angle of attack) and β (sideslip) are wind incidence angles positive as shown in figure 6 and

$$T_2 = \begin{bmatrix} \cos\beta & \sin\beta & 0 \\ -\sin\beta & \cos\beta & 0 \\ 0 & 0 & 1 \end{bmatrix} \begin{bmatrix} \cos\alpha & 0 & \sin\alpha \\ 0 & 1 & 0 \\ -\sin\alpha & 0 & \cos\alpha \end{bmatrix}$$

APPENDIX B

EQUATIONS OF MOTION AND COMPLEMENTARY RELATIONSHIPS

The six-degree-of-freedom nonlinear equations of motion are expressed in the following form:

$$\dot{\alpha} = q + \left[-\left(\frac{q_\infty S}{mV} C_X - \frac{g}{V} \sin\theta + r \sin\beta \right) \sin\alpha \right.$$

$$\left. + \left(\frac{q_\infty S}{mV} C_Z + \frac{g}{V} \cos\theta \cos\phi - p \sin\beta \right) \cos\alpha \right] \sec\beta$$

$$\dot{\beta} = -\left[\left(\frac{q_\infty S}{mV} C_X - \frac{g}{V} \sin\theta \right) \sin\beta + r \right] \cos\alpha + \left(\frac{q_\infty S}{mV} C_Y + \frac{g}{V} \cos\theta \sin\phi \right) \cos\beta$$

$$- \left[\left(\frac{q_\infty S}{mV} C_Z + \frac{g}{V} \cos\theta \cos\phi \right) \sin\beta - p \right] \sin\alpha$$

$$\frac{\dot{V}}{V} = \left(\frac{q_\infty S}{mV} C_X - \frac{g}{V} \sin\theta \right) \cos\alpha \cos\beta + \left(\frac{q_\infty S}{mV} C_Y + \frac{g}{V} \cos\theta \sin\phi \right) \sin\beta$$

$$+ \left(\frac{q_\infty S}{mV} C_Z + \frac{g}{V} \cos\theta \cos\phi \right) \sin\alpha \cos\beta$$

$$\dot{p} = \left[\left(\frac{I_Y - I_Z}{I_X} - \frac{I_{XZ}^2}{I_X I_Z} \right) qr + \left(1 - \frac{I_Y - I_X}{I_Z} \right) \frac{I_{XZ}}{I_X} pq + \frac{q_\infty Sb}{I_X} \left(C_l + \frac{I_{XZ}}{I_Z} C_n \right) \right] \frac{1}{D}$$

$$\dot{q} = \frac{q_\infty S\bar{c}}{I_Y} C_m + \frac{I_Z - I_X}{I_Y} pr + \frac{I_{XZ}}{I_Y} \left(r^2 - p^2 \right)$$

$$\dot{r} = \left[\left(\frac{I_{XZ}^2}{I_X I_Z} - \frac{I_Y - I_X}{I_Z} \right) pq + \left(\frac{I_Y - I_Z}{I_X} - 1 \right) \frac{I_{XZ}}{I_Z} qr + \frac{q_\infty Sb}{I_Z} \left(\frac{I_{XZ}}{I_X} C_l + C_n \right) \right] \frac{1}{D}$$

where $D = 1 - \dfrac{I_{XZ}^2}{I_X I_Z}$.

APPENDIX B

The aerodynamic coefficients are written in a form consistent with the data available for the most extensively tested model. Note that this results in a linear dependence upon control deflections.

$$C_X = C_X(\alpha,\beta,U=0) + C_{X_{\delta_e}}(\alpha,\beta)\delta_e$$

$$C_Y = C_Y(\alpha,\beta,U=0) + C_{Y_{\delta_e}}(\alpha,\beta)\delta_e + C_{Y_{\delta_a}}(\alpha,\beta)\delta_a + C_{Y_{\delta_r}}(\alpha,\beta)\delta_r + \frac{b}{2V}\left[C_{Y_p}(\alpha)p + C_{Y_r}(\alpha)r\right]$$

$$C_Z = C_Z(\alpha,\beta,U=0) + C_{Z_{\delta_e}}(\alpha,\beta)\delta_e$$

$$C_l = C_l(\alpha,\beta,U=0) + C_{l_{\delta_e}}(\alpha,\beta)\delta_e + C_{l_{\delta_a}}(\alpha,\beta)\delta_a + C_{l_{\delta_r}}(\alpha,\beta)\delta_r + \frac{b}{2V}\left[C_{l_p}(\alpha)p + C_{l_r}(\alpha)r\right]$$

$$C_m = C_m(\alpha,\beta,U=0) + C_{m_{\delta_e}}(\alpha,\beta)\delta_e + \frac{\bar{c}}{2V}C_{m_q}(\alpha)q$$

$$C_n = C_n(\alpha,\beta,U=0) + C_{n_{\delta_e}}(\alpha,\beta)\delta_e + C_{n_{\delta_a}}(\alpha,\beta)\delta_a + C_{n_{\delta_r}}(\alpha,\beta)\delta_r + \frac{b}{2V}\left[C_{n_p}(\alpha)p + C_{n_r}(\alpha)r\right]$$

The general relationships between the Euler angle rates and the body axis angular rates are

$$\begin{Bmatrix} \dot{\psi} \\ \dot{\theta} \\ \dot{\phi} \end{Bmatrix} = \begin{bmatrix} 0 & \sin\phi \sec\theta & \cos\phi \sec\theta \\ 0 & \cos\phi & -\sin\phi \\ 1 & \tan\theta \sin\phi & \tan\theta \cos\phi \end{bmatrix} \begin{Bmatrix} p \\ q \\ r \end{Bmatrix}$$

The requirement that the angular velocity be vertical leads to the following relationships:

$$p = -\dot{\psi} \sin\theta$$

$$q = \dot{\psi} \cos\theta \sin\phi$$

$$r = \dot{\psi} \cos\theta \cos\phi$$

with $\omega = \left|\dot{\psi}\right|$.

Using the stipulated condition that $\psi(t^*) = 0$ and expressing the linear velocity in terms of the body axes as follows allow determination of α and β in terms of θ, ϕ, γ, and ψ':

$$\begin{Bmatrix} u \\ v \\ w \end{Bmatrix} = \begin{Bmatrix} V\cos\alpha\cos\beta \\ V\sin\beta \\ V\sin\alpha\cos\beta \end{Bmatrix} = T_1(\psi{=}0,\theta,\phi) \begin{Bmatrix} V\cos\gamma\cos\psi' \\ V\cos\gamma\sin\psi' \\ -V\sin\gamma \end{Bmatrix}$$

Explicit inclusion of $\dot{V} = 0$ constraint is accomplished by solving for the speed at which $\dot{V} = 0$ given the other variables.

The resulting expression for V is

$$V = \frac{-B_V + \text{sgn } A_V\sqrt{B_V^2 - 4A_VC_V}}{2A_V}$$

where

$$A_V = \frac{1}{2}\frac{\rho S}{m}\left\{C_X\cos\alpha\cos\beta + C_Z\sin\alpha\cos\beta + \left[C_Y(\alpha,\beta,U{=}0) + C_{Y_{\delta_a}}(\alpha,\beta)\delta_a + C_{Y_{\delta_r}}(\alpha,\beta)\delta_r\right]\sin\beta\right\}$$

$$B_V = \frac{1}{2}\frac{\rho S}{m}\frac{b}{2}\left[C_{Y_p}(\alpha)p + C_{Y_r}(\alpha)r\right]\sin\beta$$

and

$$C_V = g\left[(\cos\theta\cos\phi\sin\alpha - \sin\theta\cos\alpha)\cos\beta + \cos\theta\sin\phi\sin\beta\right]$$

If additional data should be taken which result in the need for a more general functional form for the aerodynamic coefficients, an analytic solution for the velocity at which $\dot{V} = 0$ might not be possible. In this case it would probably be inadvisable to require that $\dot{V} = 0$ at each point in the search. One would then increase the dimensions of the space to be searched over from 5 to 6 and include the term $(\dot{V}/V)^2$ in the function J that is to be minimized.

The final equality constraints that are required to be satisfied at each point are $\vec{V}\cdot\hat{R} = 0$ and $V_H = R\omega$. This is accomplished by requiring that $R = (V\cos\gamma)/\omega$.

APPENDIX C

LINEARIZED EQUATIONS OF MOTION

The composition of the matrices in the following linearized system of equations will be exhibited:

$$\dot{\xi}(t) = A(t)\xi(t) + B(t)u(t)$$

where

$$\xi^T(t) = \left(\Delta\alpha, \Delta\beta, \frac{\Delta V}{V_o}, \Delta p, \Delta q, \Delta r, \Delta\theta, \Delta\phi\right)$$

The following relationships allow the matrix elements to be written more compactly:

$$q_\infty = \frac{1}{2}\rho V^2 \qquad \bar{q} = \frac{q_\infty S}{mV} \qquad D = 1 - \frac{I_{XZ}^2}{I_X I_Z}$$

$$J_1 = \frac{I_Y - I_Z}{I_X} \qquad J_2 = \frac{I_Z - I_X}{I_Y} \qquad J_3 = \frac{I_X - I_Y}{I_Z}$$

$$A_X = \bar{q}C_X \qquad A_Y = \bar{q}C_Y \qquad A_Z = \bar{q}C_Z$$

$$G_X = -\frac{g}{V}\sin\theta \qquad G_Y = \frac{g}{V}\cos\theta\sin\phi \qquad G_Z = \frac{g}{V}\cos\theta\cos\phi$$

$$a_X = A_X + G_X \qquad a_Y = A_Y + G_Y \qquad a_Z = A_Z + G_Z$$

$$T_X = \frac{q_\infty Sb}{I_X} C_l \qquad T_Y = \frac{q_\infty S\bar{c}}{I_Y} C_m \qquad T_Z = \frac{q_\infty Sb}{I_Z} C_n$$

where the coefficients are defined in appendix B.

Consider one additional point concerning the notation which will avoid a proliferation of subscripts in what is presented subsequently. It is to be understood by the reader that all partial derivatives written are to be evaluated on the nominal flight path. For example, $\frac{\partial\dot{\alpha}(t)}{\partial\alpha}$ is to be evaluated by employing values of the variables taken at time t on the nominal flight path. If the nominal flight path corresponds to an equilibrium spin condition, the partial derivatives will not, therefore, change with time.

APPENDIX C

First, the elements of matrix A are defined as follows:

$$\frac{\partial\dot{\alpha}}{\partial\alpha} = \left\{\left[-\left(a_X + r\sin\beta\right) + \frac{\partial A_Z}{\partial\alpha}\right]\cos\alpha - \left[\left(a_Z - p\sin\beta\right) + \frac{\partial A_X}{\partial\alpha}\right]\sin\alpha\right\}\sec\beta$$

$$\frac{\partial\dot{\alpha}}{\partial\beta} = (\dot{\alpha} - q)\tan\beta - p\cos\alpha - r\sin\alpha + \left(-\frac{\partial A_X}{\partial\beta}\sin\alpha + \frac{\partial A_Z}{\partial\beta}\cos\alpha\right)\sec\beta$$

$$\frac{\partial\dot{\alpha}}{\partial\left(V/V_o\right)} = \left[-\left(A_X - G_X\right)\sin\alpha + \left(A_Z - G_Z\right)\cos\alpha\right]\sec\beta$$

$$\frac{\partial\dot{\alpha}}{\partial p} = -\cos\alpha\tan\beta$$

$$\frac{\partial\dot{\alpha}}{\partial q} = 1$$

$$\frac{\partial\dot{\alpha}}{\partial r} = -\sin\alpha\tan\beta$$

$$\frac{\partial\dot{\alpha}}{\partial\theta} = \frac{g}{V\cos\beta}(\cos\theta\sin\alpha - \sin\theta\cos\phi\cos\alpha)$$

$$\frac{\partial\dot{\alpha}}{\partial\phi} = \frac{-g}{V\cos\beta}\cos\theta\sin\phi\cos\alpha$$

$$\frac{\partial\dot{\beta}}{\partial\alpha} = p\cos\alpha + r\sin\alpha + \left[\left(a_X - \frac{\partial A_Z}{\partial\alpha}\right)\sin\alpha - \cos\alpha\left(a_Z + \frac{\partial A_X}{\partial\alpha}\right)\right]\sin\beta + \frac{\partial A_Y}{\partial\alpha}\cos\beta$$

$$\frac{\partial\dot{\beta}}{\partial\beta} = -\left[\left(a_X\cos\alpha + a_Z\sin\alpha\right)\cos\beta + a_Y\sin\beta\right] + \frac{\partial A_Y}{\partial\beta}\cos\beta$$

$$- \left(\frac{\partial A_X}{\partial\beta}\cos\alpha + \frac{\partial A_Z}{\partial\beta}\sin\alpha\right)\sin\beta$$

$$\frac{\partial\dot{\beta}}{\partial\left(V/V_o\right)} = -\left\{\left[\left(A_X - G_X\right)\cos\alpha + \left(A_Z - G_Z\right)\sin\alpha\right]\sin\beta\right.$$

$$\left. - \left[\left(A_Y - G_Y\right) - \bar{q}\frac{b}{2V}\left(C_{Y_p}p + C_{Y_r}r\right)\right]\cos\beta\right\}$$

$$\frac{\partial \dot{\beta}}{\partial p} = \sin \alpha + \bar{q} \frac{b}{2V} C_{Y_p} \cos \beta$$

$$\frac{\partial \dot{\beta}}{\partial q} = 0$$

$$\frac{\partial \dot{\beta}}{\partial r} = -\cos \alpha + \bar{q} \frac{b}{2V} C_{Y_r} \cos \beta$$

$$\frac{\partial \dot{\beta}}{\partial \theta} = \frac{g}{V}\left[(\sin \theta \cos \phi \sin \alpha + \cos \theta \cos \alpha)\sin \beta - \sin \theta \sin \phi \cos \beta\right]$$

$$\frac{\partial \dot{\beta}}{\partial \phi} = \frac{g \cos \theta}{V}(\sin \phi \sin \alpha \sin \beta + \cos \phi \cos \beta)$$

$$\frac{\partial \dot{V}/V_o}{\partial \alpha} = \left[-\left(a_X - \frac{\partial A_Z}{\partial \alpha}\right)\sin \alpha + \left(a_Z + \frac{\partial A_X}{\partial \alpha}\right)\cos \alpha\right]\cos \beta + \frac{\partial A_Y}{\partial \alpha} \sin \beta$$

$$\frac{\partial \dot{V}/V_o}{\partial \beta} = -\left(a_X \cos \alpha + a_Z \sin \alpha - \frac{\partial A_Y}{\partial \beta}\right)\sin \beta + \left(a_Y + \frac{\partial A_X}{\partial \beta} \cos \alpha + \frac{\partial A_Z}{\partial \beta} \sin \alpha\right)\cos \beta$$

$$\frac{\partial \dot{V}}{\partial V} = 2\left[\left(A_X \cos \alpha + A_Z \sin \alpha\right)\cos \beta + A_Y \sin \beta\right] - \bar{q} \frac{b}{2V}\left(C_{Y_p} p + C_{Y_r} r\right)\sin \beta$$

$$\frac{\partial \dot{V}/V_o}{\partial p} = \bar{q} \frac{b}{2V} C_{Y_p} \sin \beta$$

$$\frac{\partial \dot{V}/V_o}{\partial q} = 0$$

$$\frac{\partial \dot{V}/V_o}{\partial r} = \bar{q} \frac{b}{2V} C_{Y_r} \sin \beta$$

$$\frac{\partial \dot{V}/V_o}{\partial \theta} = -\frac{g}{V}\left[(\sin \theta \cos \phi \sin \alpha + \cos \theta \cos \alpha)\cos \beta + \sin \theta \sin \phi \sin \beta\right]$$

$$\frac{\partial \dot{V}/V_o}{\partial \phi} = -\frac{g}{V} \cos \theta(\sin \phi \sin \alpha \cos \beta - \cos \phi \sin \beta)$$

$$\frac{\partial \dot{p}}{\partial \alpha} = \left(\frac{\partial T_X}{\partial \alpha} + \frac{I_{XZ}}{I_X} \frac{\partial T_Z}{\partial \alpha}\right)\frac{1}{D}$$

APPENDIX C

$$\frac{\partial \dot{p}}{\partial \beta} = \left(\frac{\partial T_X}{\partial \beta} + \frac{I_{XZ}}{I_X} \frac{\partial T_Z}{\partial \beta} \right) \frac{1}{D}$$

$$\frac{\partial \dot{p}}{\partial (V/V_o)} = \left\{ 2 \left(T_X + \frac{I_{XZ}}{I_X} T_Z \right) - \frac{q_\infty Sb}{I_X} \frac{b}{2V} \left[\left(C_{l_p} p + C_{l_r} r \right) + \frac{I_{XZ}}{I_Z} \left(C_{n_p} p + C_{n_r} r \right) \right] \right\} \frac{1}{D}$$

$$\frac{\partial \dot{p}}{\partial p} = \left[(1 + J_3) \frac{I_{XZ}}{I_X} q + \frac{q_\infty Sb}{I_X} \frac{b}{2V} \left(C_{l_p} + \frac{I_{XZ}}{I_Z} C_{n_p} \right) \right] \frac{1}{D}$$

$$\frac{\partial \dot{p}}{\partial q} = \left[\left(J_1 - \frac{I_{XZ}^2}{I_X I_Z} \right) r + (1 + J_3) \frac{I_{XZ}}{I_X} p \right] \frac{1}{D}$$

$$\frac{\partial \dot{p}}{\partial r} = \left[\left(J_1 - \frac{I_{XZ}^2}{I_X I_Z} \right) q + \frac{q_\infty Sb}{I_X} \frac{b}{2V} \left(C_{l_r} + \frac{I_{XZ}}{I_Z} C_{n_r} \right) \right] \frac{1}{D}$$

$$\frac{\partial \dot{p}}{\partial \theta} = 0$$

$$\frac{\partial \dot{p}}{\partial \phi} = 0$$

$$\frac{\partial \dot{q}}{\partial \alpha} = \frac{\partial T_Y}{\partial \alpha}$$

$$\frac{\partial \dot{q}}{\partial \beta} = \frac{\partial T_Y}{\partial \beta}$$

$$\frac{\partial \dot{q}}{\partial (V/V_o)} = 2 \left(T_Y - \frac{q_\infty S \bar{c}}{I_Y} \frac{\bar{c}}{V} C_{m_q} q \right)$$

$$\frac{\partial \dot{q}}{\partial p} = J_2 r - 2 \frac{I_{XZ}}{I_Y} p$$

$$\frac{\partial \dot{q}}{\partial q} = \frac{q_\infty S \bar{c}}{I_Y} \frac{\bar{c}}{2V} C_{m_q}$$

$$\frac{\partial \dot{q}}{\partial r} = J_2 p + 2 \frac{I_{XZ}}{I_Y} r$$

APPENDIX C

$$\frac{\partial \dot{q}}{\partial \theta} = 0$$

$$\frac{\partial \dot{q}}{\partial \phi} = 0$$

$$\frac{\partial \dot{r}}{\partial \alpha} = \left(\frac{I_{XZ}}{I_Z} \frac{\partial T_X}{\partial \alpha} + \frac{\partial T_Z}{\partial \alpha} \right) \frac{1}{D}$$

$$\frac{\partial \dot{r}}{\partial \beta} = \left(\frac{I_{XZ}}{I_Z} \frac{\partial T_X}{\partial \beta} + \frac{\partial T_Z}{\partial \beta} \right) \frac{1}{D}$$

$$\frac{\partial \dot{r}}{\partial (V/V_o)} = \left\{ 2\left(\frac{I_{XZ}}{I_Z} T_X + T_Z \right) - \frac{q_\infty Sb}{I_Z} \frac{b}{2V} \left[\frac{I_{XZ}}{I_X} \left(C_{l_p} p + C_{l_r} r \right) + \left(C_{n_p} p + C_{n_r} r \right) \right] \right\} \frac{1}{D}$$

$$\frac{\partial \dot{r}}{\partial p} = \left[\left(\frac{I_{XZ}^2}{I_X I_Z} + J_3 \right) q + \frac{q_\infty Sb}{I_Z} \frac{b}{2V} \left(\frac{I_{XZ}}{I_X} C_{l_p} + C_{n_p} \right) \right] \frac{1}{D}$$

$$\frac{\partial \dot{r}}{\partial q} = \left[\left(\frac{I_{XZ}^2}{I_X I_Z} + J_3 \right) p + \left(J_1 - 1 \right) \left(\frac{I_{XZ}}{I_Z} \right) r \right] \frac{1}{D}$$

$$\frac{\partial \dot{r}}{\partial r} = \left[\left(J_1 - 1 \right) \frac{I_{XZ}}{I_Z} q + \frac{q_\infty Sb}{I_Z} \frac{b}{2V} \left(\frac{I_{XZ}}{I_X} C_{l_r} + C_{n_r} \right) \right] \frac{1}{D}$$

$$\frac{\partial \dot{r}}{\partial \theta} = 0$$

$$\frac{\partial \dot{r}}{\partial \phi} = 0$$

$$\frac{\partial \dot{\theta}}{\partial \alpha} = 0 \qquad \frac{\partial \dot{\theta}}{\partial \beta} = 0 \qquad \frac{\partial \dot{\theta}}{\partial V} = 0$$

$$\frac{\partial \dot{\theta}}{\partial p} = 0 \qquad \frac{\partial \dot{\theta}}{\partial q} = \cos \phi \qquad \frac{\partial \dot{\theta}}{\partial r} = -\sin \phi$$

$$\frac{\partial \dot{\theta}}{\partial \theta} = 0 \qquad \frac{\partial \dot{\theta}}{\partial \phi} = -q \sin \phi - r \cos \phi$$

APPENDIX C

$$\frac{\partial\dot{\phi}}{\partial\alpha} = 0 \qquad \frac{\partial\dot{\phi}}{\partial\beta} = 0 \qquad \frac{\partial\dot{\phi}}{\partial V} = 0$$

$$\frac{\partial\dot{\phi}}{\partial p} = 1 \qquad \frac{\partial\dot{\phi}}{\partial q} = \tan\theta \sin\phi \qquad \frac{\partial\dot{\phi}}{\partial r} = \tan\theta \cos\phi$$

$$\frac{\partial\dot{\phi}}{\partial\theta} = q \sec^2\theta \sin\phi + r \sec^2\theta \cos\phi \qquad \frac{\partial\dot{\phi}}{\partial\phi} = \tan\theta(q \cos\phi - r \sin\phi)$$

Next, the elements of the matrix B are defined as follows:

$$\frac{\partial\dot{\alpha}}{\partial\delta_e} = \bar{q}\left(-C_{X_{\delta_e}} \sin\alpha + C_{Z_{\delta_e}} \cos\alpha\right)\sec\beta$$

$$\frac{\partial\dot{\alpha}}{\partial\delta_a} = 0$$

$$\frac{\partial\dot{\alpha}}{\partial\delta_r} = 0$$

$$\frac{\partial\dot{\beta}}{\partial\delta_e} = \bar{q}\left[-\left(C_{X_{\delta_e}} \cos\alpha + C_{Z_{\delta_e}} \sin\alpha\right)\sin\beta + C_{Y_{\delta_e}} \cos\beta\right]$$

$$\frac{\partial\dot{\beta}}{\partial\delta_a} = \bar{q}C_{Y_{\delta_a}} \cos\beta$$

$$\frac{\partial\dot{\beta}}{\partial\delta_r} = \bar{q}C_{Y_{\delta_r}} \cos\beta$$

$$\frac{\partial\left(\dot{V}/V_o\right)}{\partial\delta_e} = \bar{q}\left[\left(C_{X_{\delta_e}} \cos\alpha + C_{Z_{\delta_e}} \sin\alpha\right)\cos\beta + C_{Y_{\delta_e}} \sin\beta\right]$$

$$\frac{\partial\left(\dot{V}/V_o\right)}{\partial\delta_a} = \bar{q}C_{Y_{\delta_a}} \sin\beta$$

$$\frac{\partial\left(\dot{V}/V_o\right)}{\partial\delta_r} = \bar{q}C_{Y_{\delta_r}} \sin\beta$$

$$\frac{\partial\dot{p}}{\partial\delta_e} = \frac{q_\infty Sb}{I_X}\left(C_{l_{\delta_e}} + \frac{I_{XZ}}{I_Z} C_{n_{\delta_e}}\right)\frac{1}{D}$$

$$\frac{\partial\dot{p}}{\partial\delta_a} = \frac{q_\infty Sb}{I_X}\left(C_{l_{\delta_a}} + \frac{I_{XZ}}{I_Z} C_{n_{\delta_a}}\right)\frac{1}{D}$$

$$\frac{\partial \dot{p}}{\partial \delta_r} = \frac{q_\infty Sb}{I_X}\left(C_{l_{\delta_r}} + \frac{I_{XZ}}{I_Z} C_{n_{\delta_r}}\right)\frac{1}{D}$$

$$\frac{\partial \dot{q}}{\partial \delta_e} = \frac{q_\infty S\bar{c}}{I_Y} C_{m_{\delta_e}}$$

$$\frac{\partial \dot{q}}{\partial \delta_a} = 0$$

$$\frac{\partial \dot{q}}{\partial \delta_r} = 0$$

$$\frac{\partial \dot{r}}{\partial \delta_e} = \frac{q_\infty Sb}{I_Z}\left(\frac{I_{XZ}}{I_X} C_{l_{\delta_e}} + C_{n_{\delta_e}}\right)\frac{1}{D}$$

$$\frac{\partial \dot{r}}{\partial \delta_a} = \frac{q_\infty Sb}{I_Z}\left(\frac{I_{XZ}}{I_X} C_{l_{\delta_a}} + C_{n_{\delta_a}}\right)\frac{1}{D}$$

$$\frac{\partial \dot{r}}{\partial \delta_r} = \frac{q_\infty Sb}{I_Z}\left(\frac{I_{XZ}}{I_X} C_{l_{\delta_r}} + C_{n_{\delta_r}}\right)\frac{1}{D}$$

$$\frac{\partial \dot{\theta}}{\partial \delta_e} = \frac{\partial \dot{\theta}}{\partial \delta_a} = \frac{\partial \dot{\theta}}{\partial \delta_r} = 0$$

$$\frac{\partial \dot{\phi}}{\partial \delta_e} = \frac{\partial \dot{\phi}}{\partial \delta_a} = \frac{\partial \dot{\phi}}{\partial \delta_r} = 0$$

REFERENCES

1. Muse, T. C., chairman: Panel Discussion – "Where Do We Go From Here?" Presented at the Stall/Post-Stall/Spin Symposium, Wright-Patterson AFB (Ohio), Dec. 1971, pp. ZZ-1 – ZZ-25.

2. Wenglinski, T. H.: Model F-101A Results of a Steady State Spin Analysis. Rep. No. 6687 (Contract No. AF 42(600)-19284), McDonnell Aircraft Corp., Apr. 22, 1960.

3. Carter, C. V.: A Discussion of Theoretical Methods for Prediction of Spin Characteristics. Rep. No. 10732, Chance Vought Aircraft, Inc., Feb. 1957.

4. Anglin, Ernie L.; and Scher, Stanley H.: Analytical Study of Aircraft-Developed Spins and Determination of Moments Required for Satisfactory Spin Recovery. NASA TN D-2181, 1964.

5. Scher, Stanley H.; Anglin, Ernie L.; and Lawrence, George F.: Analytical Investigation of Effect of Spin Entry Technique on Spin Recovery Characteristics for a 60^{o} Delta-Wing Airplane. NASA TN D-156, 1959.

6. Grantham, William D.; and Scher, Stanley H.: Analytical Investigation and Prediction of Spin and Recovery Characteristics of the North American X-15 Airplane. NASA TM X-294, 1960.

7. Grantham, William D.; and Grafton, Sue B.: Effects of Aircraft Relative Density on Spin and Recovery Characteristics of Some Current Configurations. NASA TN D-2243, 1965.

8. Anglin, Ernie L.: Relationship Between Magnitude of Applied Spin Recovery Moment and Ensuing Number of Recovery Turns. NASA TN D-4077, 1967.

9. Davidon, William C.: Variable Metric Method for Minimization. ANL-5990 Rev. (Contract W-31-109-eng-38), Argonne Nat. Lab., Nov. 1959.

10. Fletcher, R.; and Powell, M. J. D.: A Rapidly Convergent Descent Method for Minimization. Computer J., vol. 6, no. 2, July 1963, pp. 163-168.

11. Burk, Sanger, M., Jr.; and Lee, Henry A.: Free-Spinning-Tunnel Investigation To Determine the Effect of Spin-Recovery Rockets and Thrust Simulation on the Recovery Characteristics of a 1/25-Scale Model of the Chance Vought XF8U-1 Airplane – TED No. NACA DE 392. NACA RM SL55B09, Bur. Aeronaut., 1955.

12. Grafton, Sue B.: A Study To Determine Effects of Applying Thrust on Recovery From Incipient and Developed Spins for Four Airplane Configurations. NASA TN D-3416, 1966.

13. Lusby, William A., Jr.; Nelson, Swart H.; and Hanks, Norris J.: T-38 Spin Evaluation. AFFTC-TR-61-31, U.S. Air Force, Aug. 1961.

14. Kelley, Henry J.; Denham, Walter F.; Johnson, Ivan L.; and Wheatley, Patrick O.: An Accelerated Gradient Method for Parameter Optimization With Non-Linear Constraints. J. Astronaut. Sci., vol. XIII, no. 4, July-Aug. 1966, pp. 166-169.

15. Klinar, Walter J.; Lee, Henry A.; and Wilkes, L. Faye: Free-Spinning-Tunnel Investigation of a 1/25-Scale Model of the Chance Vought XF8U-1 Airplane – TED No. NACA DE 392. NACA RM SL56L31b, Bur. Aeronaut., 1956.

16. Clexton, E. W., Jr.; Sullivan, D. A.; and Dunn, J. L.: Evaluation of the Spin and Recovery Characteristics of the F-4B Airplane. Rep. No. FT-88R-67, U.S. Naval Air Test Center (Patuxent River, Md.), Dec. 27, 1967. (Available from DDC as AD 824 914.)

17. Chambers, Joseph R.; Bowman, James S., Jr.; and Anglin, Ernie L.: Analysis of the Flat-Spin Characteristics of a Twin-Jet Swept-Wing Fighter Airplane. NASA TN D-5409, 1969.

18. Bowman, James S.; and White, William L.: Spin-Tunnel Investigation of a 1/30-Scale Model of the Fighter and Reconnaissance Versions of the McDonnell F-4B Airplane (Revised). NASA TM SX-1744, Naval Air Systems Command, 1969.

19. Bowman, James S., Jr.; and Healy, Frederick M.: Free-Spinning-Tunnel Investigation of a 1/30-Scale Model of a Twin-Jet Swept-Wing Fighter Airplane – Clearance No. N5154. NASA TM SX-446, Bur. Weapons, Dep. Navy, 1960.

20. Burk, Sanger M., Jr.; and Libbey, Charles E.: Large-Angle Motion Tests, Including Spins, of a Free-Flying Radio-Controlled 0.13-Scale Model of a Twin-Jet Swept-Wing Fighter Airplane – COORD No. N-AM-50. NASA TM SX-445, Bur. Weapons, Dep. Navy, 1961.

21. Hewes, Donald E.; and Hassell, James L., Jr.: Subsonic Flight Tests of a 1/7-Scale Radio-Controlled Model of the North American X-15 Airplane With Particular Reference to High Angle-of-Attack Conditions. NASA TM X-283, 1960.

22. Anglin, Ernie L.: Static Force Tests of a Model of a Twin-Jet Fighter Airplane for Angles of Attack From -10° to 110° and Sideslip Angles From -40° to 40°. NASA TN D-6425, 1971.

23. Grafton, Sue B.; and Libbey, Charles E.: Dynamic Stability Derivatives of a Twin-Jet Fighter Model for Angles of Attack From -10° to 110°. NASA TN D-6091, 1971.

24. Gilbert, William P.; and Libbey, Charles E.: Investigation of an Automatic Spin-Prevention System for Fighter Airplanes. NASA TN D-6670, 1972.

25. Hewes, Donald E.: Low-Subsonic Measurements of the Static and Oscillatory Lateral Stability Derivatives of a Sweptback-Wing Airplane Configuration at Angles of Attack From -10° to 90°. NASA MEMO 5-20-59L, 1959.

26. Grantham, William D.: Analytical Investigation of the Spin and Recovery Characteristics of a Supersonic Trainer Airplane Having a 24^{o} Swept Wing. NASA TM X-606, 1962.

27. Stone, Ralph W., Jr.; Burk, Sanger M., Jr.; and Bihrle, William, Jr.: The Aerodynamic Forces and Moments on a $\frac{1}{10}$-Scale Model of a Fighter Airplane in Spinning Altitudes as Measured on a Rotary Balance in the Langley 20-Foot Free-Spinning Tunnel. NACA TN 2181, 1950.

28. Chambers, Joseph R.: Status of Model Testing Techniques. Paper presented at the Stall/Post-Stall/Spin Symposium, Wright-Patterson AFB (Ohio), Dec. 1971, pp. J-1 – J-25.

29. Klinar, Walter J.; and Grantham, William D.: Investigation of the Stability of Very Flat Spins and Analysis of Effects of Applying Various Moments Utilizing the Three Moment Equations of Motion. NASA MEMO 5-25-59L, 1959.

NATIONAL AERONAUTICS AND SPACE ADMINISTRATION
WASHINGTON, D.C. 20546

OFFICIAL BUSINESS
PENALTY FOR PRIVATE USE $300

SPECIAL FOURTH-CLASS RATE BOOK

POSTAGE AND FEES PAID
NATIONAL AERONAUTICS AND SPACE ADMINISTRATION
451

U.S.MAIL

POSTMASTER: If Undeliverable (Section 158 Postal Manual) Do Not Return

"The aeronautical and space activities of the United States shall be conducted so as to contribute . . . to the expansion of human knowledge of phenomena in the atmosphere and space. The Administration shall provide for the widest practicable and appropriate dissemination of information concerning its activities and the results thereof."

—NATIONAL AERONAUTICS AND SPACE ACT OF 1958

NASA SCIENTIFIC AND TECHNICAL PUBLICATIONS

TECHNICAL REPORTS: Scientific and technical information considered important, complete, and a lasting contribution to existing knowledge.

TECHNICAL NOTES: Information less broad in scope but nevertheless of importance as a contribution to existing knowledge.

TECHNICAL MEMORANDUMS: Information receiving limited distribution because of preliminary data, security classification, or other reasons. Also includes conference proceedings with either limited or unlimited distribution.

CONTRACTOR REPORTS: Scientific and technical information generated under a NASA contract or grant and considered an important contribution to existing knowledge.

TECHNICAL TRANSLATIONS: Information published in a foreign language considered to merit NASA distribution in English.

SPECIAL PUBLICATIONS: Information derived from or of value to NASA activities. Publications include final reports of major projects, monographs, data compilations, handbooks, sourcebooks, and special bibliographies.

TECHNOLOGY UTILIZATION PUBLICATIONS: Information on technology used by NASA that may be of particular interest in commercial and other non-aerospace applications. Publications include Tech Briefs, Technology Utilization Reports and Technology Surveys.

Details on the availability of these publications may be obtained from:

SCIENTIFIC AND TECHNICAL INFORMATION OFFICE

NATIONAL AERONAUTICS AND SPACE ADMINISTRATION

Washington, D.C. 20546